THE INFLUENCE ON THE FATIGUE STRENGTH OF ALUMINIUM ALLOY PARTS OF THE RELATIONSHIP BETWEEN THE SURFACE RESIDUAL STRESS STATE AND THE LOAD-INDUCED STRESS STATE

B. Jaensson

Saab-Scania AB, S-581 88 Linköping, Sweden

ABSTRACT

To be able to make a reasonable assessment of the fatigue strength improvement attainable by shot peening one must know how the cyclic stresses should be added to the residual stresses and which failure criterion should be used.

The vector-addition method of stress superposition, used by Mattson and Roberts (1958), has been applied in a laboratory test program comprising fatigue testing of aluminium alloy specimens, shot peened under five different levels of preload. The fatigue strength, evaluated at $N=10^7$ cycles, was found to satisfy the octahedral shear stress criterion in three cases, viz. normal shot peening and peening under two levels of compressive preload. The corresponding failure mechanism was shear mode crack propagation from an iniation point below the surface. Tensile strain peened specimens failed by normal mode crack propagation inwards from a subsurface initiation point. This behaviour implied deviation from the shear stress failure criterion.

The results of this investigation allow judgements to be made as to which areas of a fatigue-critical part are amenable to improvement by shot peening and which are not.

KEYWORDS

Fatigue strength, aluminium alloy, shot peening, strain peening, stress state, residual stress distribution.

INTRODUCTION

The principal reason why shot peening is applied to metallic machine or vehicle components is the endeavour of raising the fatigue strength or increasing the part's reliability under fatigue conditions. Although shot peening is widely used, methods of quantifying its beneficial influence are seldom discussed.

Sines (1959) published a compilation of fatigue data obtained for different materials under different combinations of static and alternating stress.

His conclusion was, that the permissible amplitude of the octahedral shear stress is linearly related to the sum of the orthogonal normal static stresses. For material close to a free surface this criterion can be represented by a series of concentric ellipses in a diagram over alternating longitudinal stress vs. alternating transverse stress for failure in N cycles, the size of the ellipses decreasing with increasing sum of static stresses.

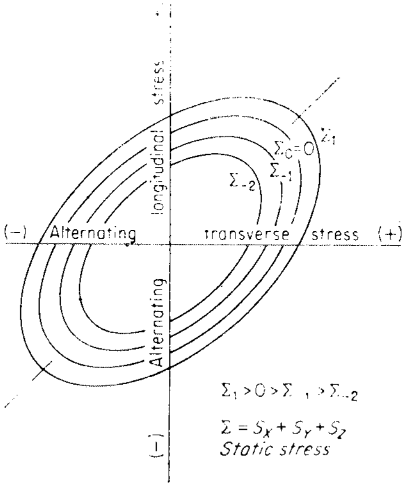

Fig. 1. Fatigue failure criterion according to Sines (1959)

Moreover, Sines contended that this form of the failure criterion is valid for macroscopic residual stresses as well as for static load-induced stresses, i.e. compressive residual stresses are favourable, irrespective of their orientation.

In contrast to this, Mattson and Roberts (1958) in an investigation concerning the influence of strain peening on the bending fatigue strength of spring steel attempted to rationalize their results by testing the vector sum of the residual and the load-induced stresses against different failure criteria.

A third paper should be mentioned, the findings of which are pertinent to the investigation which will be reported here. After push-pull testing of shot peened aluminium 7075 fatigue specimens Was and Pelloux (1979) found that the crack initiation site was below the surface layer affected by peening, at a depth of ca. 400 µm. From initiation to break-through of the surface, the crack had propagated in stage I (shear) mode.

EXPERIMENTAL

The practical significance of the way the cyclic stresses are added to the static, residual stresses lies in the assessment of the shot peening effects at various locations of the metal part being designed for a certain fatigue life. In most cases the surface stress state due to shot peening can be considered rotationally symmetric, while the load-induced stress state normally is more or less uniaxial.

In a laboratory research program devised to test the influence of the stress state relationship, the type of load-induced stress state was kept constant, while the axial-tangential residual stress ratio was varied. This was accomplished by shot peening the unnotched fatigue specimens under different degrees of compressive or tensile prestress.

The material used for the investigation was a high strength aluminium alloy AA 7009, containing the following percentages of alloying elements: Zn 5, Mg 2.5, Cu 1, Ag 0.3, Cr 0.2. The hour-glass-shaped fatigue specimens (length 96 mm, minimum diameter 8 mm, K_t = 1.08) were taken in the longitudinal direction of a hand forging, aged to the T 73 condition.

To keep the specimens under compressive or tensile load during shot peening a three-legged, strain gauge instrumented steel fixture was used. The shot peening was done with S 230 steel shot to an Almen A intensity of 0,20-0,22 mm and 150 % coverage.

Residual stress measurements were made using a computer-controlled X-ray diffractometer[1] with centerless (residual stress) goniometer, equipped with facilities for keeping the angle of measurement (ψ) constant, independent of Bragg angle 2θ (Jaensson, 1980). During each stress measurement, comprising four ψ angles from 0° to 45°, the specimen was rotated, with or without the preload fixture.

Four levels of prestressing the specimens during peening were used (in addition to normal peening): -300 MPa, -150 MPa, +150 MPa, and +300 MPa. On two specimens of each series, comprising 13 - 15 pieces, stress measurements were made after machining, after preloading, after peening - under preload, after peening - without preload. The remaining fatigue specimens were measured only after the peening operation was completed.

On three specimens, shot peened under zero, +300 MPa and -300 MPa preload, respectively, the variation of axial and tangential stresses with depth was determined. Corrections for the influence of stress gradient and of removed layers were applied (Evans, 1971).

The fatigue testing was done in Amsler high frequency pulsators with a stress ratio R = 0.1.

RESULTS

In Fig. 2 the results of stress measurements before and after shot peening are given for one specimen of each preload level. Fig. 3 shows the influence of preload on the axial and tangential residual stresses. The values stated are averages from 14 - 17 specimens each. Residual stress distributions are shown in Fig. 4. Average residual stress data are given in Table 1 together with corresponding fatigue limits for $N = 10^7$ cycles. The crack inition depth under the surface, as determined by scanning electron microscopy on long-life specimens, is given in Table 2.

---

[1] Rigaku Strainflex MSF

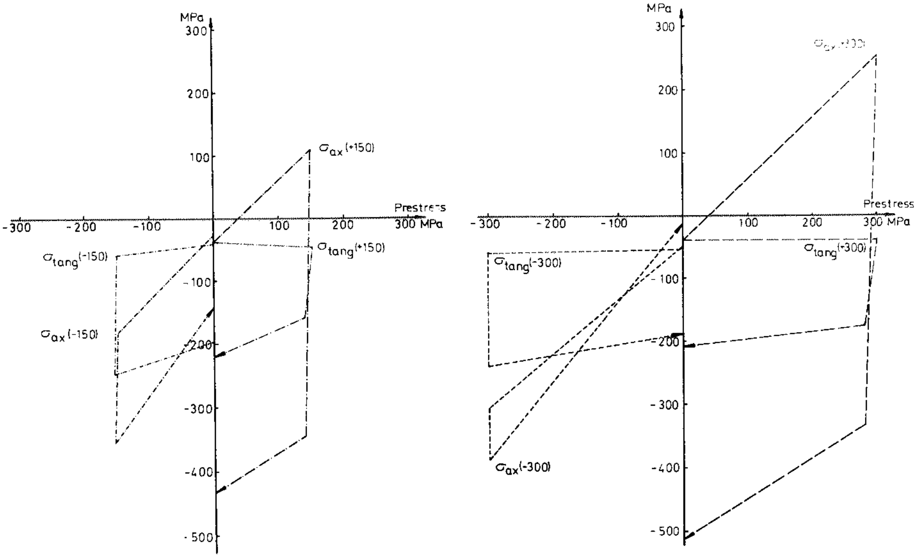

Fig. 2. The development of axial and tangential stresses through the strain peening process.

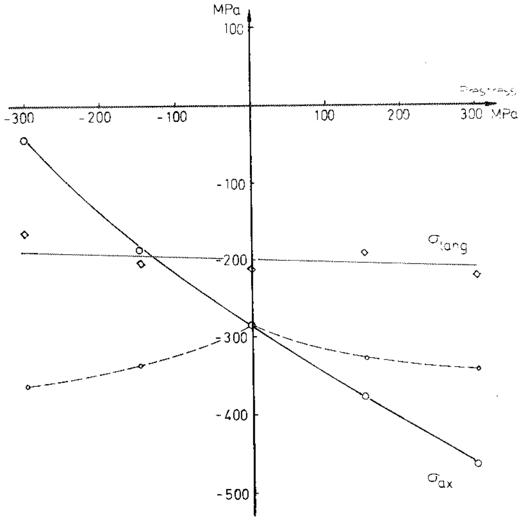

Fig. 3. Residual stresses due to shot peening as a function of prestress level. (Broken line: axial stresses measured on specimens still under preload.)

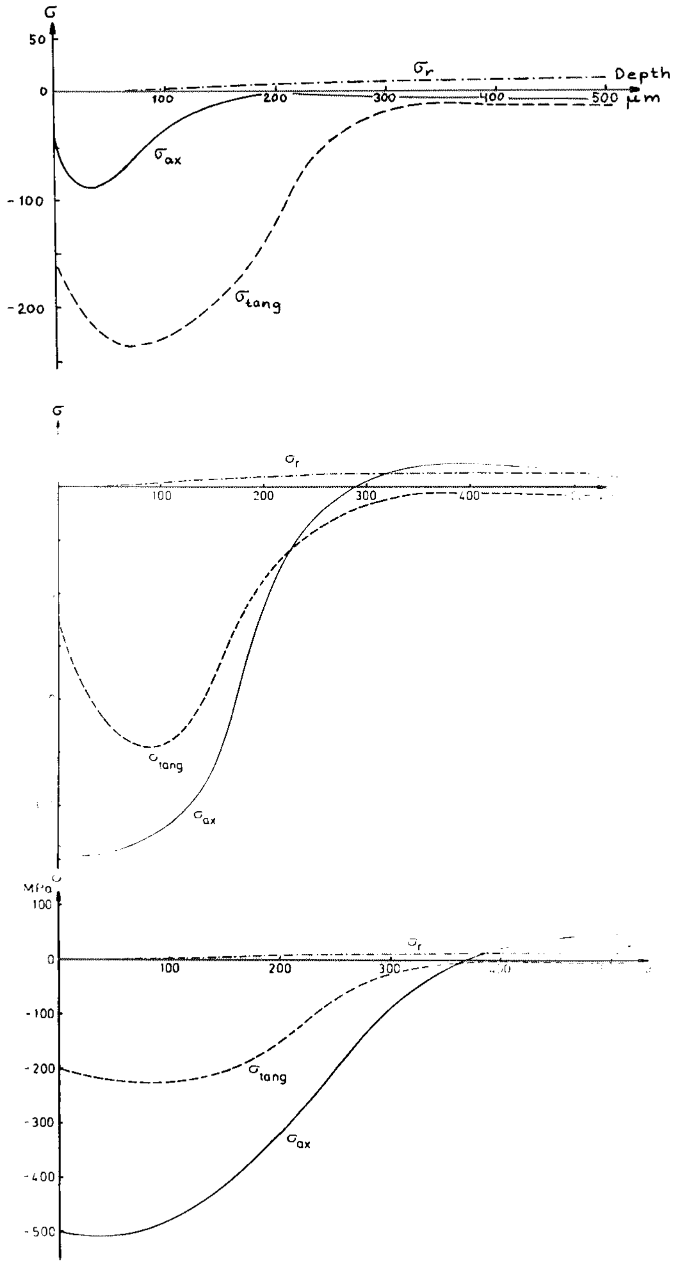

Fig. 4. Residual stress distributions representing prestress levels -300, 0, and +300 MPa.

TABLE 1 RESIDUAL STRESS MEAN VALUES FOR DIFFERENT PRESTRESS LEVELS. MAXIMUM CYCLIC STRESS FOR $N = 10^7$ CYCLES. ALL STRESSES ARE GIVEN IN MPa

Prestress	-300	-150	0	+150	+300
σ_{ax}	- 41	-185	-284	-378	-465
σ_{tang}	-164	-201	-209	-187	-221
$\sigma_{max}(10^7)$	140	195	275	340	340

TABLE 2 CRACK INITIATION DEPTH UNDER SPECIMEN SURFACE

Prestress	MPa	-300	-150	0	+150	+300
Depth	µm	150-200	350-400	400-500	650-800	800-900

DISCUSSION

It appears from Fig. 2 that the more positive the axial preload stress, the greater is the peening-induced change in the direction of compressive stress. The axial compressive stress level, determined after shot peening but under preload, is highest for the extreme preload levels (± 300 MPa), lowest in the case of zero preload (normal peening). This is evident from Fig. 3 (broken line; based on two specimens at each preload level $\neq 0$).

In the series of residual stress distributions both similarities and dissimilarities can be found. For all three preload levels studied here the tangential compressive stress had declined within 300 µm below the surface. In contrast to this, the axial compressive stress depth varies from 150 µm (-300 MPa prestress) to 450 µm (+300 MPa prestress). In the latter case neither the axial nor the tangential stress distribution has a marked peak below the surface.

In Fig. 5 the residual stress states after shot peening under the five preload levels have been plotted in a σ_{ax} - σ_{tang}-diagram. Each point forms the origin of a vector representing the fatigue failure stress (σ_{max}) for $N = 10^7$ cycles. Also an octahedral shear stress ellipse has been drawn, the size of which has been adjusted to fit the fatigue results for the preload levels -300, -150, and 0 MPa. The other two vectors are strongly displaced in the direction of compressive axial stresses.

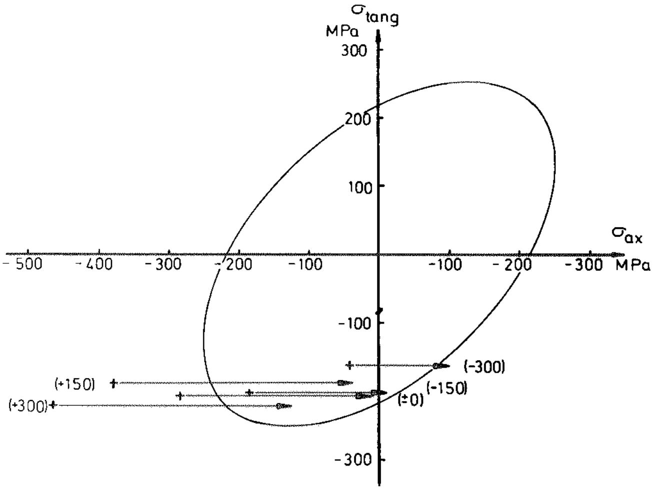

Fig. 5. Stress diagram showing residual stress state due to shot peening (+), vectors representing maximum cyclic stress, and ellipse illustrating the octahedral shear stress criterion.

The first-mentioned group of results can be rationalized by the following course of events.

The crack initiation occurs below the surface, behind the compressive peak in axial residual stress (cf. Fig. 4 and Table 2). Crack propagation in shear mode (stage I) to the surface is the critical phase, which determines the maximum stress level for the fatigue life considered. Due to elastic restraint from the surrounding material the crack describes a zigzag path, with only very small shear facets. (Fig. 6 a).

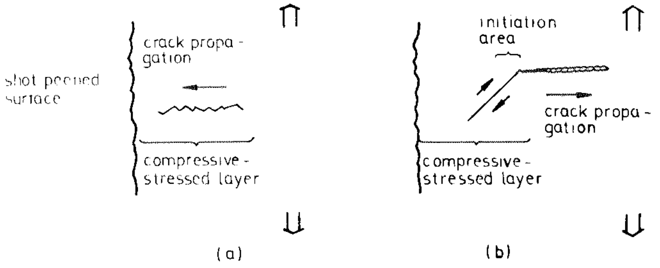

(a) (b)

Fig. 6. Development of internal shear mode crack (a) and of mixed-mode crack (b) (schematically).

The fatigue specimens shot peened under tensile preload are thought to have failed in the following way.

> The crack initiation area is on the rear side of the residual stress peak. Due to the high level of the resulting tensile stress behind the peak the crack will propagate by two simultaneous mechanisms: in the shear mode outwards, in the tensile mode inwards. The shear mode propagation is no longer critical. - In well-defined cases the following description applies.
>
> The combined action of two crack branches, inclined 45° and 90° to the loading direction, respectively, results in a characteristic appearance of the initiation area (cf. Figs. 6b and 7). On one hand the 90° branch alleviates the elastic restraints, thus permitting a macroscopic shear facet to be formed. On the other hand the existence of a shear crack facilitates the tensile mode propagation.

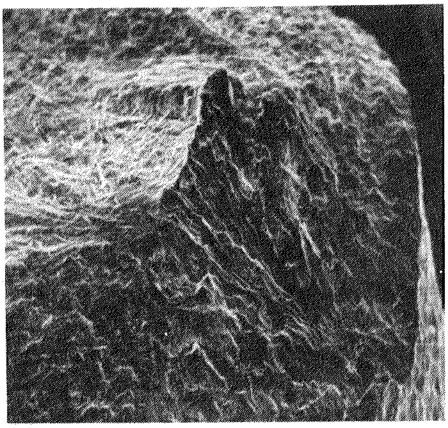

Fig. 7. Crack initiation region in a specimen shot peened under +150 MPa prestress.

Considering the influence on the fatigue strength of increasing tensile preload during shot peening it is found that the gradual appearance of a second failure mechanism limits the attainable gains.

In the light of the proposed failure mechanisms the following comments to Fig. 5 should be made.

For the two cases of shot peening under tensile preload the σ_{max} vector foot-points should be displaced close to the origin of the diagram. The octahedral shear stress criterion should be modified to one based on maximum normal stress.

In those cases when shear mode crack growth is the fatigue critical event (in this investigation shot peening under 0, -150 and -300 MPa prestress, respectively) the relevant residual stress state changes with time, from crack initiation. The plotted vector origins represent the final phase, when the crack front penetrates the surface. Also the location of the shear stress ellipse changes slightly, however, in correspondence with the varying radial stress level (Fig. 4).

For design purposes, the main significance of the vector-addition method in conjunction with the octahedral shear stress criterion is, that it is possible to decide which areas of the part under consideration will benefit from the introduction of residual compressive stresses and which will not.

Normally, shot peening will yield a rotationally symmetric surface stress state, i.e. the foot-point of the vector representing the cyclic stress lies in the third quadrant of the stress diagram, close to the 45° line through the origin. It is evident, that the most favourable type of load-induced stress state is the purely biaxial one, since the 45° direction gives maximum distance between the foot-point and critical parts of the shear stress ellipse.

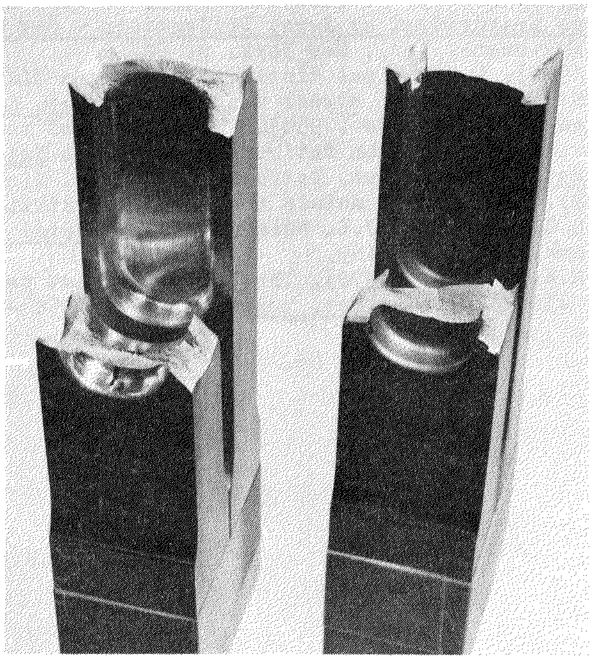

Fig. 8. Fatigue specimens, as-machined and shot-peened, with I-beam cross section. Crack initiation points are indicated.

As an illustrative example, consider the two broken I-beam test pieces in Fig. 8. Two series of specimens, as-machined and shot peened, were fatigue tested at different maximum stress levels, with stress ratio R = -0.3. By shot peening, the fracture initiation point was consistently displaced from the intended zone at the end of the recess to one of the flanges. The significant difference between these two locations is supposed to be that the load-induced stress is uniaxial in the flange, making this site to a lesser degree amenable to fatigue strength improvement by shot peening than the double-curved part of the recess, where the load-induced surface stresses are biaxial.

ACKNOWLEDGEMENTS

The author would like to express his gratitude to C. Westerlund and B. Forslind for their skilful assistance in doing the shot peening - X-ray diffraction work (C.W.) and fatigue testing (B.F.).

Also, Saab-Scania AB:s permission to publish this paper is gratefully acknowledged.

REFERENCES

Evans, W.P. (1971). Effects of removed layers. In M.E. Hilley (Ed.), Residual Stress Measurement by X-ray Diffraction - SAE J784a. Society of Automotive Engineers, Inc., New York. p. 62.

Jaensson, B. (1980). A principal distinction between different kinds of X-ray equipment for residual stress measurement. Mat. Sci. Eng., 43, 169-176

Mattson, R.L. and J.G. Roberts (1958). The effects of residual stresses induced by strain peening upon fatigue strength. In Internal Stresses and Fatigue in Metals. Symposium. Detroit and Warren, Mich. pp. 337-357.

Sines, G. (1959). Behavior of metals under complex static and alternating stresses. In G. Sines and J.L. Waisman (Eds.), Metal Fatigue. Mc Graw-Hill, New York. pp. 145 - 169.

Was, G.S. and R.M. Pelloux (1979). The effect of shot peening on the fatigue behavior of alloy 7075-T6. Met. Trans. A, 10 A, 656 - 658.